At some distance downstream of the shock which is to be determined, the equilibrium ionization level ϵ_{eq} is reached. Under equilibrium conditions $ud\epsilon/dx = 0$, $\epsilon = \epsilon_{eq}$, and $T \equiv T_e$; thus Eq. (6) reduces to the well-known Saha equation.

The remaining equation relating the two temperatures T and T_e obtained by considering the conservation of energy for electrons is[4]

$$T^* = T_e^* + \frac{K(1 + \frac{3}{2}T_e^*)T_e^{*3}[(T_{exc}/T_e) + 2]\exp(-T_{exc}/T_e)[(1 - \epsilon) - \rho^*\epsilon^2 T_e^{*-3/2}e^{1/T_e^*}]}{\epsilon \ln(DT_e^{*3}/\rho^*\epsilon)} \quad (8)$$

where $T^* = T/T_{ion}$, and, for argon, $K = 1.53 \times 10^4$ and $D = 0.2980$.

Two-Temperature Analysis of Nonequilibrium Region

The variation of ϵ with x in the nonequilibrium region can be found from Eqs. (6) and (1); thus,

$$x = \int_{\epsilon_i}^{\epsilon} \frac{(u/U)d\epsilon}{\frac{A}{U}\epsilon\left[\frac{T_{exc}}{T_e} + 2\right]\frac{U}{u}\frac{\rho_0}{\rho_{ion}}\left(\frac{T_e}{T_{ion}}\right)^{3/2}\exp\left[\frac{T_{ion}}{T_e} - \frac{T_{exc}}{T_e}\right]\left\{(1 - \epsilon)e^{-T_{ion}/T_e} - \epsilon^2\frac{\rho_0}{\rho_{ion}}\frac{U}{u}\left(\frac{T_{ion}}{T_e}\right)^{3/2}\right\}} \quad (9)$$

In Eq. (9), the lower limit of integration, ϵ_i, is the initial value of the degree of ionization upstream of the shock. The thickness of the nonequilibrium ionization region, x, can be defined conveniently by using $\epsilon = 0.99\epsilon_{eq}$ for the upper limit of integration. The equilibrium value of the ionization, ϵ_{eq}, is obtained from Saha's equation for the given conditions.

To facilitate the numerical integration, it is desirable to write Eq. (9) in a more convenient form. Thus, combining Eqs. (1–5), the velocity ratio can be written as

$$\frac{u}{U} = \frac{5}{8}\left\{1 - \left[1 - \left(\frac{4}{5}\right)^2\left(\frac{\lambda - \epsilon}{\lambda}\right)\right]^{1/2}\right\} \quad (10)$$

where

$$\lambda = mU^2/2kT_{ion} \quad (11)$$

It is seen that the parameter λ is a measure of the strength of the shock, since it is the ratio of the kinetic energy of the freestream to the ionization energy of the gas.

It only remains to determine the corresponding values of T_e, T, and ϵ to be used in the range of integration. This is accomplished by combining Eqs. (1, 2, and 5) to get

$$T = \frac{mU^2}{k}\left[\frac{u}{U} - \left(\frac{u}{U}\right)^2\right] - T_e\epsilon \quad (12)$$

Using Eqs. (7) and (10) and equating the right-hand sides of Eqs. (12) and (8) gives an expression relating T_e and ϵ. For a series of values of ϵ in the range of integration, corresponding values of electron temperatures T_e can thus be calculated; Eq. (12) can then be used to calculate the corresponding atom (ion) temperatures T.

The numerical integration of Eq. (9) can be carried out using the corresponding values of T_e and ϵ, the results of which give the function $x = x(\epsilon)$. That is, Eq. (9) has the form

$$x^* = \int_{\epsilon_i}^{\epsilon} F(\epsilon)d\epsilon \quad (13)$$

where the dimensionless distance

$$x^* = \frac{A(\rho_0/\rho_{ion})x}{U} = \frac{A(\rho_0/\rho_{ion})x}{(2\lambda kT_{ion}/m)^{1/2}} = \frac{A(\rho_0/\rho_{ion})x}{(2\lambda)^{1/2}v_{ion}} \quad (14)$$

The parameter v_{ion} is the characteristic velocity of the gas ($v_{ion} = 2.0209 \times 10^4$ fps for argon). Once the function $x(\epsilon)$ is known, the values of all other physical variables can be found from Eqs. (1, 5, and 10).

Results

The integration of Eq. (9) has been carried out for argon for a series of strong shock conditions. Typical results for the calculations are shown in Fig. 1.

In general, it is only necessary to specify the shock strength λ, the freestream density parameter ρ_0/ρ_{ion}, and the gas. For the results shown in Fig. 1, the shock strength was specified as $\lambda = 1$, and the freestream density parameter was chosen as $\rho_0/\rho_{ion} = 1.7 \times 10^{-7}$. These given conditions, used in conjunction with Saha's equation and Eqs. (1, 10, and 12), yield the downstream equilibrium ionization level $\epsilon_{eq} = 0.59$. The initial degree of ionization was taken as $\epsilon_i = 0.001$.

The results show that, for the given freestream conditions, equilibrium is reached at a distance of 0.075 in. downstream of the shock. Over the first two-thirds of the nonequilibrium region, there is very little change in the shock parameters; rapid changes in pressure, density, and atom (ion) temperature occur in the latter third.

Perhaps the most interesting and surprising result is that, for all practical purposes, the electron temperature remains constant at the equilibrium value throughout the nonequilibrium region. The use of the assumption of a constant electron temperature at the equilibrium value would represent a considerable simplification in the two-temperature analysis of the nonequilibrium region behind strong shocks.

References

[1] Bray, K. N. C. and Wilson, J. A., "A preliminary study of ionic recombination of argon in wind tunnel nozzles," Rept. 134, Dept. Aeronaut. Astronaut., Univ. Southampton, Hampshire, England (1960).

[2] Truitt, R. W. and Perkins, J. N., "Thermodynamics of the ideal r-times ionized monatomic gas," *Developments in Mechanics* (Plenum Press, New York, 1961), Vol. 1.

[3] Freeman, N. C., "Dynamics of a dissociating gas, III, Nonequilibrium theory," AGARD, NATO Rept. 133 (July 1957).

[4] Bray, K. N. C. and Wilson, J. A., "A preliminary study of ionic recombination of argon in wind tunnel nozzles, Part II," TN 11, Dept. Aeronaut. Astronaut., Univ. Southampton, Hampshire, England (1961).

Self-Preservation in Fully Expanded Round Turbulent Jets

FREDERICK P. BOYNTON*
General Dynamics/Astronautics, San Diego, Calif.

IT is well established that radial velocity profiles obtained at different axial locations in the fully developed region of subsonic, constant-density, axially symmetric, turbulent, free jets issuing into a stagnant medium can be normalized to congruent curves by plotting them in the proper reduced coordinates. Townsend's book,[1] for example, shows that, when the velocity (u) measured at a given radial distance

Received June 27, 1963.

* Senior Research Engineer, Space Science Laboratories Member AIAA.

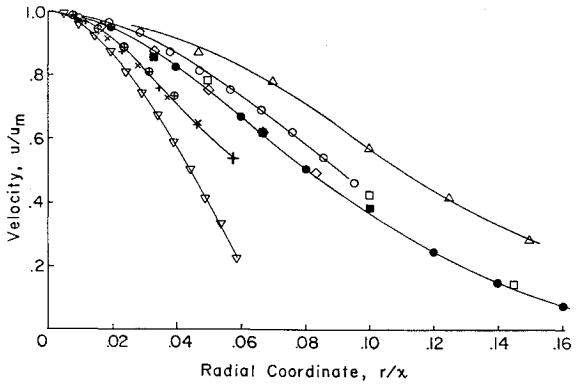

Fig. 1 Similarity plot of velocity profiles in real coordinates.

(r) from the centerline of the jet is divided by the velocity on the axis (u_m) and plotted as a function of the radial distance divided by the quotient of the axial distance (x) and a proportionality constant (σ), all points obtained beyond a certain axial distance from the origin of the jet fall on a universal curve. Such self-preserving flows cannot exist in the "real" coordinate system when significant density variations occur in the flow field, though an approximate similarity is observed if σx is replaced by the jet half-radius ($r_{1/2}$).[2-4] A suggestion has recently been made[5] that variable-density flows may be self-preserving in the Howarth-Dorodnitsyn[6] coordinates, where a transformation of the type

$$R = \left[2\int_0^r \left(\frac{\rho}{\rho_e}\right) r'dr'\right]^{1/2} \qquad (1)$$

where ρ is the density at a point and ρ_e is the ambient density, is used to convert the momentum and continuity equations to their incompressible form.

Data from several sources have been compared in order to test this hypothesis and to attempt to establish the values of the constant σ. The data examined include those obtained in the following kinds of jets: 1) low speed and constant density[1]; 2) low speed, heated, and of uniform molecular weight[2]; 3) low speed, constant temperature, and with molecular weight different from the ambient medium[3]; and 4) supersonic ($M = 1.74$ and $M = 2.60$),[4,7] initially isoenergetic, and of uniform molecular weight. Although the available data do not cover the range of variables of interest in all applications of jet mixing theory, there is enough spread to allow one to determine whether the hypothesis of self-preservation in transformed coordinates is in reasonable accord with known facts.

In Fig. 1 the velocity profiles are plotted in the usual fashion, i.e., as u/u_m vs r/x (see Table 1 for symbols). These data, although exhibiting an approximate similarity among like sets of profiles, do not cross-correlate well. A jet of less dense fluid than the ambient medium exhibits a broader velocity profile than a constant-density jet, and a jet of denser fluid has a sharper profile. The jets of high Mach number have very sharp profiles. In Fig. 2 the data are plotted in a coordinate system in which the transformation, Eq. (1), has been employed. The differences among the low-speed jets

Table 1 Explanation of symbols used in graphs

Symbol	M	Jet fluid	Jet temp.	x/D (Figs. 1 and 2)	Ref.
●	$\ll 1$	Air	amb.	8–20	1
○	$\ll 1$	Air	569°K	15	2
□	$\ll 1$	N_2	amb.	16, 24	3
◇	$\ll 1$	CO_2	amb.	24	3
△	$\ll 1$	He	amb.	16	3
+×⊕	1.74	Air	183.5°K	14.6, 17.8, 21.9	4
▽	2.6	Air	124°K	20	7

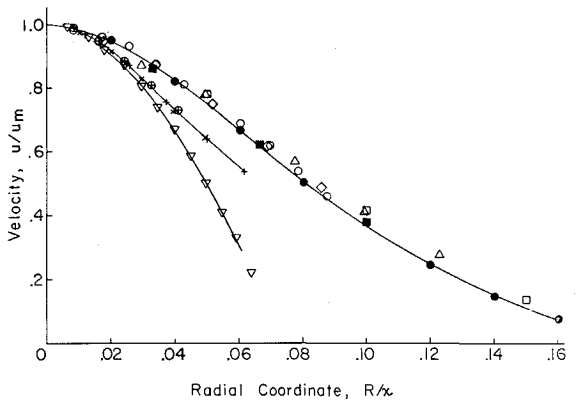

Fig. 2 Similarity plot of velocity profiles in transformed coordinates.

are greatly reduced, and one is tempted to ascribe these differences to experimental error.†

The tendency of the supersonic jets to spread less than the low-speed jets is not resolved by the transformation alone. It is necessary also to postulate that the spreading constant σ is a function of Mach number, being 1 at $M = 0$ and increasing as M increases. A choice of $\sigma = 1.268$ for the Mach 1.74 jet and 1.535 for the Mach 2.60 jet brings these curves into good agreement with the other data. It may be significant that these numbers represent the square root of the ratio of the initial (jet nozzle exit) total enthalpies to the initial static enthalpies, where

$$H_p/h_p = 1 + \tfrac{1}{2}(\gamma - 1)M_p^2 \qquad (2)$$

This ratio is also the ratio of the rms random molecular velocity to the rms total molecular velocity. The significance of this finding cannot be assessed without more data.

A similarity analysis applied to the transformed momentum equation leads to the conclusion that, in the fully developed region,

$$u_m = u_p(\rho_e/\rho_p)I_{11}^{-1/2}\sigma r_p/x \qquad (3)$$

where

$$I_{11} = 2\int_0^\infty f_1^2(\eta)\eta d\eta$$

$\eta = r\sigma/x$, and $f_1(\eta)$ is the universal function represented by the low-speed data in Fig. 2. (For Townsend's[1] equation for f, $I_{11} = \frac{1}{4}$.) In Fig. 3 there is shown a plot of the centerline velocity vs the normalized axial coordinate. It is shown that the correspondence is reasonably good, except that there appears to be some residual density variation in the low-speed jets. Perhaps the density has an effect upon the virtual origin of the flow.

The equation of transport of a scalar quantity (heat or mass) in a round jet may also be transformed by use of Eq.

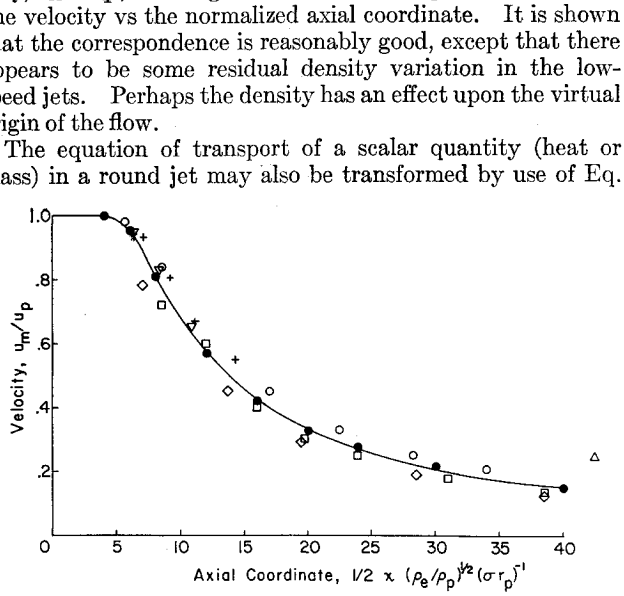

Fig. 3 Axial velocity decay.

† The temptation is particularly strong when one recognizes that the carefully obtained data[1,2] correlate very well.

(1). Some data[2, 3, 8] have been examined to determine whether a universal similarity exists for these profiles, but the results are inconclusive.

The results of this investigation imply that the Howarth transformation may be employed to reduce all fully developed jet velocity data to a common scale if a spreading constant that is a function of the Mach number is employed. It is possible this constant is simply related to the ratio of nozzle static and total enthalpies.

References

[1] Townsend, A. A., *The Structure of Turbulent Shear Flow* (Cambridge University Press, Cambridge, 1956), pp. 182–186.

[2] Corsin, S. and Uberoi, M. S., "Further experiments on the flow and heat transfer in a heated turbulent air jet," NACA Rept. 998 (1950).

[3] Keagy, W. R. and Weller, A. E., "A study of freely expanding inhomogeneous jets," *1949 Heat Transfer and Fluid Mechanics Institute* (American Society of Mechanical Engineers, New York, May 1949), pp. 89–98.

[4] Rietdijk, J. A., "Metingen aan Vrije Supersone Stralen," Ph.D. Thesis, De Technische Hogeschool te Delft, The Netherlands (1960); derived data presented with Broer, L. J. F., "Measurements on supersonic free jets," Appl. Sci. Res. A9, 465–477 (1960).

[5] Snyder, W. T., "The use of the Howarth transformation in turbulent, compressible flow," J. Aerospace Sci. 29, 235–236 (1962).

[6] Howarth, P. L., "Concerning the effect of compressibility on laminar boundary layers and their separation," Proc. Roy. Soc. (London) **194**, 16–42 (1948).

[7] Pitkin, E. T. and Glassman, S., "Experimental mixing profiles of a Mach 2.6 free jet," J. Aerospace Sci. **25**, 791 (1958).

[8] Hinze, J. O. and van der Hegge Zijnen, B. G., "Transfer of heat and matter in the turbulent mixing zone of an axially symmetric jet," Appl. Sci. Res. **A1**, 435–461 (1949).

Some Effects of Surface Roughness on the Turbulent Boundary Layer

O. E. Tewfik*

Corning Glass Works, Corning, N.Y.

It is well known that the turbulent boundary layer is sensitive to surface roughness.[1] The increase in skin friction due to various types of surface roughness is reviewed concisely in Ref. 2. This note describes the results of measurements of the effects of a special type of surface roughness peculiar to woven-wire porous materials on some overall characteristics of the turbulent boundary layer such as skin friction and boundary-layer growth, as well as on the detailed structure of the boundary layer such as the velocity and shear stress distributions throughout the boundary layer. This type of porous materials frequently is used in investigations of mass-transfer cooling and many recent engineering applications.

In fabricating the porous material, the weaving and calendaring processes resulted in the formation of regular triangular depressions in its surface of about 0.005 in. to the side and approximately of the same depth. A sheet of the material was rolled into a 2-in.-o.d. circular cylinder and fitted with a suitable nosepiece and afterbody. The assembly, with its axis parallel to the tunnel air stream, was mounted in the 1- × 2-ft low-speed wind tunnel of the Heat Transfer Laboratory. The model, apparatus, and nomenclature are described in detail in Ref. 3. Velocity profiles were measured at various axial locations, from which the boundary layer thickness, displacement thickness, and momentum thickness were determined. By extrapolating these thicknesses to zero, the effective starting point of the boundary layer was

Received July 1, 1963. Communication from the Heat Transfer Laboratory, University of Minnesota, Minneapolis, Minn. The contribution of L. S. Jurewicz, Assistant Research Officer at the National Research Council, Canada, in measuring all velocity profiles is gratefully acknowledged. This research was supported partially by the U. S. Air Force through the Air Force Office of Scientific Research of the Air Research and Development Command under Contract AF 49(638)-558.

* Project Engineer. Member AIAA.

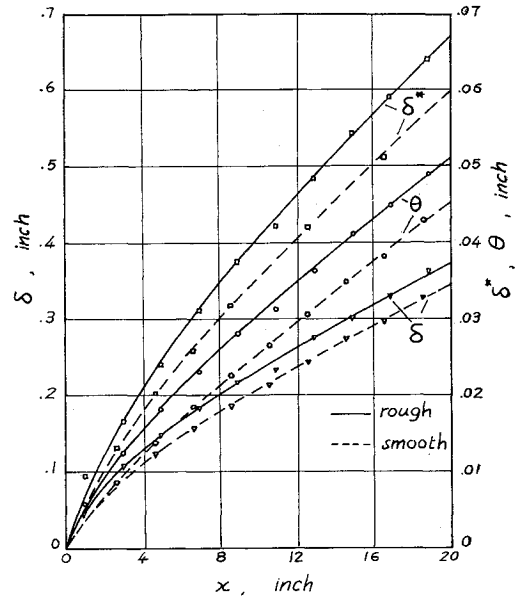

Fig. 1 Boundary layer growth.

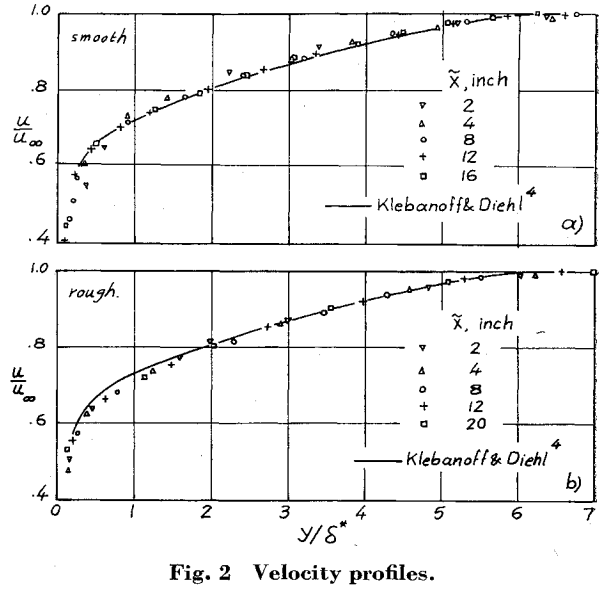

Fig. 2 Velocity profiles.

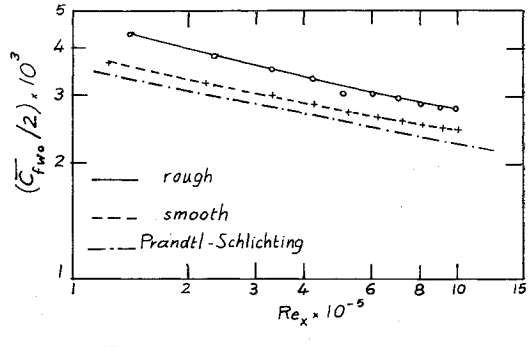

Fig. 3 Average skin friction.